Published in final edited form as:
Dev Cell. 2013 December 23; 27(6): 635–647. doi:10.1016/j.devcel.2013.11.011.

Long-Chain Acyl CoA Synthetase 4A regulates Smad activity and dorsoventral patterning in the zebrafish embryo

Rosa Linda Miyares[1,2,6], **Cornelia Stein**[3,6], **Björn Renisch**[3], **Jennifer Lynn Anderson**[2], **Matthias Hammerschmidt**[3,4,5,*], and **Steven Arthur Farber**[2,*]

[1]Department of Biology, Johns Hopkins University, Baltimore, MD 21218, USA

[2]Department of Embryology, Carnegie Institution for Science, Baltimore, MD 21218, USA

[3]Institute of Developmental Biology, University of Cologne, D-50674 Cologne, Germany

[4]Center for Molecular Medicine Cologne, University of Cologne, D-50931 Cologne, Germany

[5]Cologne Excellence Cluster on Cellular Stress Responses in Aging-Associated Diseases (CECAD), University of Cologne, D-50674 Cologne, Germany

Summary

Long-chain polyunsaturated fatty acids (LC-PUFA) and their metabolites are critical players in cell biology and embryonic development. Here we show that long-chain acyl CoA synthetase 4a (Acsl4a), an LC-PUFA activating enzyme, is essential for proper patterning of the zebrafish dorsoventral axis. Loss of Acsl4a results in dorsalized embryos due to attenuated Bmp signaling. We demonstrate that Acsl4a modulates the activity of Smad transcription factors, the downstream mediators of Bmp signaling. Acsl4a promotes the inhibition of p38 MAPK and the Akt-mediated inhibition of glycogen synthase kinase 3 (GSK3), critical inhibitors of Smad activity. Consequently, introduction of a constitutively active Akt can rescue the dorsalized phenotype of Acsl4a deficient embryos. Our results reveal a critical role for Acsl4a in modulating Bmp-Smad activity and provide a potential avenue for LC-PUFAs to influence a variety of developmental processes.

Introduction

Fatty acids (FA) play essential roles in the cell as sources of energy, membrane components, and signaling molecules. Any FA can be converted into energy, but long-chain polyunsaturated FAs (LC-PUFA) such as arachidonic acid (AA), eicosapentaenoic acid (EPA), and docosahexaenoic acid (DHA) also play critical roles in membrane fluidity and as precursors of signaling molecules such as eicosanoids (Bazan, 2006; Grossfield et al., 2006; Kitajka et al., 2002; Stillwell et al., 2005). Acyl-CoA synthetase enzymes convert free FAs to fatty acyl-CoAs as the initial step in a majority of FA processing events. There are numerous vertebrate long-chain acyl-CoA synthetase (ACSL) enzymes, each with differences in binding affinity for free long-chain FAs, tissue expression, and/or subcellular localization (Coleman et al., 2000). ACSL4 is unique among the characterized Acyl-CoA

*Correspondence: farber@ciwemb.edu (S.F.), matthias.hammerschmidt@uni-koeln.de (M.H.).
6These authors contributed equally to this work

synthetase enzymes, in that it has a strong preference for AA and EPA over other long-chain FAs (Cao et al., 1998; Kang et al., 1997; Stinnett et al., 2007).

Mutations in ACSL4 homologs implicate fundamental roles in cell function and embryonic development. Human mutations cause X-linked mental retardation and heterozygous female carriers have extremely skewed X-inactivation, indicating a survival advantage for cells expressing the wild-type allele (Longo et al., 2003; Meloni et al., 2002b; Raynaud et al., 2000; Yonath et al., 2011). Likewise, heterozygous female mice display compromised uterus development and fertility, and only very rarely transmit the disrupted allele to offspring (Cho, 2001). Finally, *Drosophila* mutants are recessive lethal (McQuilton et al., 2012) and hypomorphs display defects in segmentation (Zhang et al., 2011) and development of the CNS (Gazou et al., 2013; Liu et al., 2011; Meloni et al., 2002a; Meloni et al., 2009; Piccini et al., 1998; Zhang et al., 2009). However, the molecular underpinnings of these phenotypes have yet to be described.

In this report, we demonstrate a requirement for Acsl4a in dorsoventral patterning of the zebrafish embryo and elucidate the molecular mechanisms underlying this effect. The vertebrate dorsoventral axis is patterned by a gradient of bone morphogenetic proteins (Bmp), members of the TGFβ superfamily of secreted growth factors. Bmps bind transmembrane type I/type II serine/threonine kinase receptor complexes, which phosphorylate serine residues at the C-terminus of receptor-regulated Smad transcription factors (R-Smad; Smad1,5,8). R-Smads are the intracellular proteins that transduce the extracellular Bmp signal to the nucleus and regulate gene transcription (Macias-Silva et al., 1996).

In zebrafish, the ventral-to-dorsal Bmp gradient is set up step-wise. Zygotic *bmp2b* and *bmp7a* expression is initiated by the maternally supplied Bmp member Gdf6a (Sidi et al., 2003; Wilm and Solnica-Krezel, 2003), mediated by maternally and zygotically supplied Smad5 (Hild et al., 1999; Kramer et al., 2002), followed by a refinement of the gradient involving positive Bmp auto-regulation on the ventral side (Hammerschmidt et al., 1996b; Kishimoto et al., 1997; Nguyen et al., 1998) and by the dorsal secretion of Bmp inhibitors (reviewed in De Robertis and Kuroda, 2004; Hammerschmidt and Mullins, 2002; Little and Mullins, 2006; Schier and Talbot, 2005).

While this linear Bmp signaling pathway has been well described, recent studies suggest that R-Smads can integrate inputs from other signaling pathways known to profoundly influence embryogenesis. For example, Fibroblast Growth Factor (FGF) and Wnt signaling modulate R-Smad activity by regulating phosphorylation of a central linker region of the R-Smad protein (Fuentealba et al., 2007; Sapkota et al., 2007). FGF signals via a mitogen-activated protein kinase (MAPK), which phosphorylates four conserved consensus sites (PXSP) (Kretzschmar et al., 1997; Sapkota et al., 2007). Canonical Wnt signaling acts via inhibition of glycogen synthase kinase 3 (GSK3) (He et al., 1995), which phosphorylates R-Smad after it has been primed by MAPK phosphorylation (Fuentealba et al., 2007; Sapkota et al., 2007). Together, MAPK and GSK3 phosphorylation of R-Smad leads to binding of Smurf E3 ubiquitin ligases, polyubiquitination and proteasomal degradation, thus turning off Bmp signaling (Fuentealba et al., 2007; Sapkota et al., 2007; Zhu et al., 1999).

In the present study, we demonstrate that Acsl4a regulates Bmp R-Smad activity and thus is essential for dorsoventral patterning. Disruption of Acsl4a induces a dorsalized phenotype, resulting from its unexpected role in maintaining proper levels of activated R-Smad transcription factors. We unravel the molecular mechanism underlying this effect, demonstrating that Acsl4a is required to inhibit p38 MAPK and Akt-dependent GSK3 activity, thereby attenuating R-Smad linker phosphorylation and promoting R-Smad

stability. Our data implicate LC-PUFA metabolism in R-Smad regulation and vertebrate dorsoventral patterning.

Results

Identification of zebrafish ACSL4 orthologs

To search for ACSL4 orthologs, we queried the zebrafish genome assembly with the human ACSL4 protein sequence, revealing two genes, *acsl4a* and *acsl4l*. We confirm that these genes are orthologous to the mammalian *ACSL4* gene based on synteny (Figure S1A) and protein sequence homology (Figure S1B). Zebrafish Acsl4a best matches the characterized ACSL4 proteins (Figure S1B-D). A residue important for AA activation (Stinnett et al., 2007) is conserved in Acsl4a and lost in Acsl4l (Figure S1C). Furthermore, Acsl4a contains the N-terminal region of the brain specific human ACSL4 splice isoform (Meloni et al., 2002a) (Figure S1D).

Consistent with our hypothesis that LC-PUFA metabolism is essential during early embryogenesis, whole mount mRNA *in situ* hybridization revealed maternal *acsl4a* transcript (Figure 1A). Zygotic expression initiates at the beginning of gastrulation (germ ring stage, 5.5 hpf; Figure 1A). During gastrula stages, *acsl4a* is highly expressed in the yolk syncytial layer (YSL) (Figure 1A), an early segregating cell lineage important for the uptake of yolk nutrients as well as secretion of signaling molecules (reviewed in Carvalho and Heisenberg, 2010). In addition, *acsl4a* is expressed in the developing CNS (Figure S1E), consistent with the observation that Acsl4a orthologs impact brain function (Meloni et al., 2002a; Zhang et al., 2009).

Acsl4a plays a role in dorsoventral patterning

For Acsl4a loss-of-function studies, we designed two translation-blocking antisense morpholinos (MO) to the 5′ untranslated region (UTR) of the *acsl4a* transcript. Loss of Acsl4a results in significant dorsalization of zebrafish embryos (Figures 1B–H, S1E–I and S2A–D; see Figure S2A–D for a comparison of MO1 and MO2). The morphology of *acsl4a* morphants resembles that of mutations in ventral specifying *bmp* genes (Mullins et al., 1996); both show a loss of ventrally-derived tissues, such as blood, pronephros and tail, and the expansion of dorsal tissues, such as notochord and somites, resulting in the trunk twisting upon itself (Figure 1B).

These morphological changes were preceded by corresponding shifts in the expression domains of ventral- and dorsal-specific genes (Figure 1C) during gastrula (Figures 1D–G) and segmentation stages (Figures 1H–I, S1E–H). At mid-gastrula stages (80% epiboly; 8.5 hpf), *acsl4a* morphants display strong ventral expansion of the expression domains of *tbx6* (Figure 1D, S2B) in dorsal (paraxial) mesoderm and *foxb1.2* (Figure 1F) in dorsal (neuro) ectoderm, both of which extend around the entire circumference of the embryos and fuse ventrally. In contrast, expression of *eve1*, a marker of ventral mesoderm (Figure 1E) and *gata2*, a marker of ventral ectoderm (Figure 1G), are lost *acsl4a* in morphant embryos. During segmentation stages, expansion of dorsal derivatives is evident in the neural plate (increased width of the midbrain-hindbrain boundary and of hindbrain rhombomeres 3 and 5: Figures 1H, S1E–G, S2A), somites (Figure 1I) and notochord (Figure S1I). Conversely, ventral derivatives such as the pronephros (Figure 1H), otic placode (Figures 1H, S1G), and blood (Figure S2C, D) are absent or strongly reduced.

Overexpression of *acsl4a* has the opposite effect—ventralization, characterized morphologically by a decrease or absence of the head and notochord and the expansion of the blood island (Figure 1B) (Fisher et al., 1997; Hammerschmidt et al., 1996b). To confirm

that the enzymatic activity of Acsl4a contributes to the ventralized phenotype, we mutated a conserved amino acid in zebrafish Acsl4a that was shown to be essential for catalytic activity of rat ACSL4 (Stinnett et al., 2007). Overexpression of the catalytically inactive Acsl4a (Acsl4aCI) produced morphologically wild-type embryos (Figure 1B). In addition, injection of *acsl4a* mRNA (lacking the 5′UTR targeted by the MOs) diminished the dorsalized phenotype caused by *acsl4a* MO ($p < 0.05$; Figure S2E,F), indicating that the effects caused by the *acsl4a* MO and mRNA are specific.

Two lines of evidence suggest that it is the maternally deposited *acsl4a* mRNA that mediates the effect on dorsoventral patterning. First, in contrast to the translation-blocking MOs, three splice-blocking MOs gave no discernible dorsoventral defects (Figure S2G and data not shown). Translation-blocking MOs inhibit both maternal and zygotic mRNA (Heasman et al., 2000; Nasevicius and Ekker, 2000), whereas splice-blocking MOs do not inhibit maternal mRNA (which is stored as spliced, mature transcripts). Second, we directly targeted the zygotic *acsl4a* transcripts by exploiting their restricted expression in the YSL. Injecting a translation-blocking MO directly into the extraembryonic YSL had no effect on dorsoventral patterning, in contrast to injection into the 1–4 cell stage (Figure S2H).

Acsl4a alters the *bmp* gradient

The Bmp gradient governing dorsoventral patterning involves both maternally and zygotically supplied factors (Hammerschmidt and Mullins, 2002). To assess whether maternally supplied Acsl4a is involved in early steps of Bmp gradient formation, we performed *bmp* expression analysis at a late-blastula stage (30% epiboly; 4.5 hpf). Injection of an *acsl4a* MO disrupts the ventral to dorsal *bmp2b* and *bmp7a* gradient whereas overexpression of Acsl4a results in elevated and ectopic dorsal *bmp* expression (Figure 2A,B). During gastrulation (80% epiboly; 8.5hpf), when the dorsoventral axis is being patterned, we see a decrease in *bmp2b* and *bmp7a* expression (1.5 and 1.6 fold respectively, $p<0.0005$; RNA-seq) in *acsl4a* MO-injected embryos. Corresponding changes were observed for C-terminal phosphorylated (activated) Smad1/5 ($pSmad^{C\text{-}term}$), a direct read-out for Bmp signaling (Tanimoto et al., 2000). As early as late blastula stages (sphere; 4hpf), when $pSmad^{C\text{-}term}$ levels in wild-type embryos are relatively low, there is a significant reduction in *acsl4a* MO-injected embryos (Figures 2C, S3A). At shield stage (6 hpf), this reduction is even more pronounced (Figures 2C, S3B). Moreover, immunohistochemistry reveals a lack of $pSmad^{C\text{-}term}$ in ventral nuclei of *acsl4a* morphants (Figure 2D). In contrast to an almost complete loss of $pSmad^{C\text{-}Term}$, total Smad1/5/8 levels are only partially reduced in shield-stage *acsl4a* morphants (Figures 2C, S3A,B). Together, these data indicate that the dorsalization of *acsl4a* morphants is due to a reduction in the Bmp gradient and diminished Bmp signaling.

Acsl4a plays a role in Bmp signal reception/transduction

The early alterations in *bmp* expression observed in Acsl4a morphants are similar to those previously reported for embryos lacking maternal supply of the TGFβ ligand Radar/Gdf6a (Sidi et al., 2003) or maternal supply of Smad5 (Kramer et al., 2002). Furthermore, Bmps exhibit positive feedback on the transcription of their own genes (e.g. Kishimoto et al., 1997; Nguyen et al., 1998). Therefore, the reduced *bmp* expression levels observed in *acsl4a* morphants could result either from attenuated levels of Bmp ligands or an impaired ability to respond to Bmp. To help distinguish between these two possibilities, we performed cell transplantation experiments (Figure 2E). Upon transplantation into wild-type hosts, *acsl4a* morphant cells lack $pSmad^{C\text{-}term}$ staining, whereas directly adjacent wild-type cells show normal levels (Figure 2E, middle panel). Bmps have been shown to act both in an autocrine (Nikaido et al., 1999) and a paracrine fashion (Kishimoto et al., 1997; Nguyen et al., 1998), with cells receiving Bmp ligand that is secreted both by themselves and by adjacent cells.

Therefore, we conclude that isolated *ascl4a* morphant cells are incapable of processing paracrine Bmp signals from their wild-type neighbors, indicative of a role for Ascl4a at the level of Bmp signal reception or transduction. Conversely, wild-type cells transplanted into *acsl4a* MO-injected hosts are positive for $pSmad^{C\text{-}term}$ staining, whereas morphant neighbors are not (Figure 2E, bottom panel). While these data illustrate that wild-type cells are capable of processing Bmp signals in an Acsl4a-depleted environment, normalized $pSmad^{C\text{-}term}$ staining intensities are reduced to 51.9 ± 7.5% of the intensities of wild-type cells transplanted into wild-type hosts ($p< 0.0005$; compare top and bottom panels of Figure 2E). This effect is most likely due to reduced *bmp* expression in *acsl4a* morphant host cells, thus resulting in compromised paracrine Bmp signaling to the transplanted wild-type cells. In sum, the results of the transplant studies suggest a role for Ascl4a in Bmp signal reception and/or transduction.

Acsl4a acts downstream of Bmp receptor activation to regulate R-Smad activity

To study whether Acsl4a interferes with Bmp signal transduction at the level of receptor activation, we tested the effects of a constitutively active (CA) version of the type I receptor, Alk8 (Alk8 Q204D) (Bauer et al., 2001) on the *acsl4a* morphant phenotype. Type I receptors bearing this modification activate signal transduction and phosphorylate R-Smad proteins in the absence of Bmp ligands (Wieser et al., 1995). To quantify the extent of dorsalization, we measured the angle of dorsal mesodermal marker *tbx6* expression in late gastrulae (described in Figure 3A). *acsl4a* MO-injected embryos have a significantly ($p<.0001$) expanded angle of *tbx6* expression (Figure 3B,C). Combining Acsl4a depletion with Alk8CA overexpression resulted in similarly dorsalized embryos (Figure 3B,C). We obtained comparable results when we assessed dorsoventral patterning by morphological criteria at later developmental stages (24 hpf); in contrast to loss of Acsl4a, the loss of Bmp2b was efficiently rescued by *alk8CA* mRNA (Figure S4). Furthermore, Western blots at sphere (Figure 3D) and at shield stage (Figure 3E) revealed a robust increase of $pSmad^{C\text{-}Term}$ levels after injection of *alk8CA* mRNA (2^{nd} lanes). However, there is little to no $pSmad^{C\text{-}Term}$ immunoreactivity in *acsl4a* MO morphants overexpressing Alk8CA (4^{th} lanes). Collectively, our findings indicate a role for Acsl4a in regulating the intracellular Bmp signaling cascade, downstream of type I receptors.

Acsl4a mediates its effect on R-Smad activity via linker phosphorylation

R-Smads are both positively and negatively regulated by phosphorylation events (Figure 4A). R-Smads are activated by Bmp-receptor mediated phosphorylation (Macias-Silva et al., 1996), whereas linker phosphorylation by MAPKs and GSK3 leads to proteasomal degradation (Fuentealba et al., 2007; Sapkota et al., 2007; Zhu et al., 1999). Thus, the loss of $pSmad^{C\text{-}term}$ in *acsl4a* morphants may be due to 1) failure of Bmp receptor-mediated phosphorylation or 2) degradation following linker phosphorylation. To distinguish between these two possibilities, we asked whether either bypassing Bmp receptor-mediated phosphorylation or preventing linker phosphorylation of R-Smad could rescue the *acsl4a* morphant phenotype. To bypass Bmp receptor-mediated phosphorylation, we utilized a constitutively active, phosphomimetic Smad5 (Smad5PM), in which the C-terminal serine targets of the Bmp receptor (SSVS) are replaced with aspartate residues. To abolish linker phosphorylation, we generated a MAPK-resistant Smad5 ($Smad5^{\Delta MAPK}$) by mutating the serine residues of the four MAPK target sequences to alanines (PXSP→PXAP; Figures 4A, S5A).

Overexpression of Smad5 (Figure S5C) or Smad5PM (Figure 4B,C) fails to rescue the *acsl4a* morphant's dorsalized phenotype, although they are slightly less dorsalized than *acsl4a* MO alone. This is in striking contrast to the effects of MAPK-resistant Smad5 (Figure 4B,C). When combined with *acsl4a* MO, $smad5^{\Delta MAPK}$ mRNA not only rescues the

dorsalized phenotype of *acsl4a* MO, it results in ventralization (Figure 4B,C). Importantly, this outcome is not due to *smad5*$^{\Delta MAPK}$ having a stronger ventralizing ability than *smad5PM*, as we confirmed that the mRNAs had comparable ventralizing effects with parallel injections into wild-type controls (Figure S5D,E). This shows that the R-Smad linker phosphoresidues are essential for the dorsalized phenotype of *acsl4a* morphants. To confirm that the loss of Smad signaling is due to linker phosphorylation and subsequent ubiquitin-mediated degradation of R-Smad, we examined C-terminal phosphorylation of Smad5$^{\Delta MAPK}$ and a degradation-resistant Smad5 lacking the Smurf binding site (Figure S5B; Smad5$^{\Delta Smurf}$). Both constructs are phosphorylated by the Bmp receptor in an Acsl4a-independent manner (Figure S5F). Together, these data support a model where Acsl4a promotes Bmp signal transduction by inhibiting R-Smad linker phosphorylation and consequently proteasomal degradation.

Acsl4a regulates p38 MAPK activity and Smad1/5 linker phosphorylation

There are three major MAPK family members, extracellular signal-regulated kinases (Erk), c-Jun N-terminal kinases (JNK) and p38 kinases, all of which have been shown to be capable of phosphorylating and inhibiting Bmp R-Smads (Fuentealba et al., 2007; Kamaraju and Roberts, 2005; Mori et al., 2004). To investigate whether Acsl4a affects MAPK activity, we utilized phosphospecific antibodies to assess levels of activated MAPK (Figure 5A) or the upstream MAPKK. Indeed, we found a significant increase in activated p38 MAPK levels in *acsl4a* MO-injected embryos (4±0.9 fold, $p<0.01$, n=6; Figure 5B) between high and sphere stages (3.5–4 hpf). In contrast, levels of activated Erk1/2 and MKK4, the MAPKK upstream of JNK, are not increased in *acsl4a* MO-injected embryos (Figure S6A,B).

In order to determine if activation of p38 MAPK results in the phosphorylation of the R-Smad linker, we utilized an antibody created to recognize MAPK phosphorylated R-Smad (Fuentealba et al., 2007). Endogenous levels of MAPK phosphorylated R-Smad could not be detected from zebrafish embryo lysates (Figure S6C), presumably because Smad1/5 is rapidly ubiquitinated by Smurf E3 ligases (Zhu et al., 1999) and degraded following linker phosphorylation (Figure 4A). Hence, in order to stabilize R-Smad, we utilized the aforementioned Smad5 construct lacking the Smurf binding site (PPPAY) (Figure S5B). Using this stabilized Smad5$^{\Delta Smurf}$, we visualized a marked increase in MAPK phosphorylation in *acsl4a* morphants (9.7±4.5 fold increase over Smad5$^{\Delta Smurf}$ alone, $p<0.05$, n=5; Figure 5D). This indicates that during normal development, Acsl4a inhibits p38 activity and thereby the (destabilizing) linker phosphorylation of Smad1/5.

Acsl4a regulates Akt and GSK3 activity, and constitutively active Akt rescues the dorsoventral defects of *acsl4a* morphant embryos

Linker-mediated degradation of Bmp R-Smad involves sequential phosphorylation by MAPK and GSK3 (Fuentealba et al., 2007; Sapkota et al., 2007) (Figure 4A). Therefore, we next asked whether loss of Acsl4a also affects the activity of GSK3. GSK3 is regulated by multiple means, including inhibitory phosphorylation by Akt (also called protein kinase B; PKB) at Ser^{21} (GSK3α) and Ser^{9} (GSK3β) (Cross et al., 1995; Medina and Wandosell, 2011). Western blot analysis with a phosphospecific antibody against phosphorylated Ser$^{21/9}$ GSK3 (Figure 6A) revealed a strong decrease in inhibitory GSK3 phosphorylation in shield stage (6 hpf) *acsl4a* morphants compared to controls, while total GSK3β levels remained unaltered (Figure 6B,E). In addition, Akt activity is significantly reduced in *acsl4a* morphant embryos (Figure 6D,E).

To investigate whether these alterations in Akt/GSK3 activity are relevant to Acsl4a's role in dorsoventral patterning, we utilized a constitutively active form of Akt (AktCA) (Kohn et

al., 1996). Notably, injection of *aktCA* mRNA leads to increased GSK3 inhibition in *acsl4a* morphants (Figure 6F), while reducing the *acsl4a* MO-induced expansion of dorsal mesoderm to wild-type conditions (Figure 6G,H). This indicates that in addition to inhibiting p38, Acsl4a promotes the phosphorylation and activation of Akt, thereby decreasing GSK3 activity. Moreover, AktCA can compensate for the loss of Acsl4a to restore GSK3 inhibition, Bmp signaling and proper dorsoventral patterning.

Discussion

Recently, researchers uncovered that during dorsoventral axis patterning the Bmp signaling pathway is integrated with other classical signaling pathways at the level of the R-Smad transcription factors (Fuentealba et al., 2007; Eivers et al., 2008; Eivers et al., 2009; Hashiguchi and Mullins, 2013). FGF and Wnt signaling, which are also implicated in dorsoventral patterning of the zebrafish embryo (Fürthauer et al., 2004; Lekven et al., 2001), regulate kinases (MAPK and GSK3, respectively) that phosphorylate Bmp R-Smads on a central linker region, ultimately leading to degradation through the ubiquitin/proteasome system. We have found that Acsl4a, an LC-PUFA activating enzyme, is essential for proper patterning of the zebrafish dorsoventral axis through its ability to suppress inhibitory linker phosphorylation of R-Smads by mechanisms that likely act in parallel to FGF and Wnt signaling (Figure 7).

We provide evidence that Acsl4a influences both the establishment and zygotic refinement of the Bmp gradient through its impact on the R-Smad transcription factor. Like the Bmp receptor, Alk8 (Mintzer et al., 2001), the Bmp-related ligand, Gdf6a (Sidi et al., 2003) and the transcription factor, Smad5 (Hild et al., 1999; Kramer et al., 2002), *acsl4a* transcripts are maternally provided. Loss of Acsl4a results in a dramatic reduction of active R-Smad proteins capable of mediating Bmp signal transduction. Further, this reduction occurs prior to the defects caused by loss of Bmp2b and Bmp7a ligands. These data suggest that Acsl4a interferes with the transduction of maternally supplied signals like Gdf6a (Sidi et al., 2003) to set up the early Bmp2b/Bmp7a gradient. Acsl4a may also interfere with the zygotic refinement of the Bmp gradient, involving positive Bmp2b/Bmp7a autoregulation. Our transplant studies point to a cell autonomous role for Acsl4a in maintaining the signaling pool of R-Smad proteins, which is in contrast to the non-cell autonomous effect previously described for the Bmp2b ligand (Nguyen et al., 1998). Furthermore, a constitutively active version of the type I receptor Alk8, which readily ventralizes *bmp2b* morphants, fails to do so in *acsl4a* morphants. Together, these data indicate that Acsl4a must interfere with intracellular Bmp signal transduction at the level of R-Smad activity.

We provide several lines of evidence that Acsl4a attenuation results in the loss of activated R-Smad due to linker-mediated degradation. We show that in contrast to constitutively active Smad5 (Smad5PM), overexpression of Smad proteins that lack the MAPK consensus phosphorylation sites (Smad5$^{\Delta MAPK}$) or the binding site for the E3 ubiquitin ligase (Smad5$^{\Delta Smurf}$) can rescue the levels of pSmad$^{C\text{-}Term}$ and revert the dorsoventral patterning defects of the *acsl4a* morphants. In addition, using the Smad$^{\Delta Smurf}$ construct, we revealed a dramatic increase in MAPK-mediated R-Smad linker phosphorylation in *acsl4a* MO-injected embryos. Total R-Smad levels were significantly decreased only at later/gastrula stages, which may reflect both degradation of signaling pools of R-Smad as well as a decrease in zygotic Smad expression. Indeed, Smad1 and Smad8/Smad9 mRNA levels are significantly decreased in *acsl4a* morphant embryos at 80% epiboly (1.24 and 1.58 fold respectively $p<0.0005$; RNA-seq).

Of the three major MAPK family members (p38, Erk1/2, MKK4/JNK), each implicated in dorsoventral patterning (Bradham and McClay, 2006; Fürthauer et al., 2004; Keren et al.,

2008; Pera, 2003; Rui et al., 2007), only activated p38 levels were significantly increased in *acsl4a* morphants. This increase occurred at high stage, consistent with the timing of Smad5 linker phosphorylation and the reduction of both $pSmad^{C\text{-}Term}$ and *bmp* expression levels in *acsl4a* morphants. Although p38 MAPK family members have been implicated mainly in non-canonical Bmp/TGFβ signaling and TGFβ R-Smad inhibition (reviewed in Kamato et al., 2013; Zhang, 2009), they have also have a role in the dorsoventral patterning of *Xenopus* mesoderm (Keren et al., 2008).

GSK3 activity can be regulated at multiple levels. Signaling by canonical Wnts leads to GSK3 inhibition via the modulation of GSK3/axin/APC/Dishevelled multi-protein complexes. Another pathway involves Akt/PKB, which inhibits GSK3 via phosphorylation at $Ser^{21/9}$ (Medina and Wandosell, 2011). At shield stage, when Bmp patterns the dorsoventral axis, *acsl4a* morphants displayed significant reductions both in phosphorylated (active) Akt and in $Ser^{21/9}$-phosphorylated (inactive) GSK3 levels. However, these changes were not evident at sphere stage (data not shown), when we saw strong p38 MAPK activation.

Our data demonstrating that a constitutively active version of Akt (Kohn et al., 1996) can rescue the *acsl4a* morphant phenotype further supports a model whereby both p38 MAPK and Akt/GSK3 work downstream of Acsl4a to regulate R-Smad stability. For the three kinases to act in a single linear pathway, p38 would need to activate GSK3 or inhibit Akt. However, studies have shown that p38 inhibits GSK3 (e.g. Thornton et al., 2008) or activates Akt (e.g. Perdiguero et al., 2011). Therefore, and in light of the temporal differences between the change in p38 and Akt activity observed in the *acsl4a* morphants, we favor a model where Acsl4a regulates p38 and Akt in parallel pathways. Inhibition of p38 initiates Smad1/5 stabilization and this effect is maintained by later Akt-mediated inhibition of GSK3 activity. While the literature on Akt is extensive, there is little prior work linking it to dorsoventral patterning.

Our observation linking Acsl4a and R-Smad regulation may be the basis of the defects observed in *Drosophila Acsl* mutants (Zhang et al., 2009; Zhang et al., 2011). Intriguingly, the segmentation defects in *Drosophila acsl* mutants (Zhang et al., 2011) resemble those of Mad (the Smad1/5 homolog) depletion (Eivers et al., 2009). Moreover, *Drosophila* Mad is phosphorylated by MAPK and GSK3 in segmental patterns and this phosphorylation is required for proper segment patterning (Eivers et al., 2009).

In addition to the Bmp R-Smads (Smad1/5/8), the Activin/Nodal/TGFβ-regulated Smads (Smad2/3) are inhibited by linker phosphorylation (Funaba et al., 2002; Kretzschmar et al., 1999). We did not examine levels of Smad2/3 phosphorylation in *acsl4a* morphants. However, we showed that Smad2/3-dependent Nodal signaling (Jia et al., 2008) is unaffected, evidenced by the normal expression of the Nodal-dependent mesodermal marker *ntl* (Feldman et al., 1998; Gritsman et al., 1999) (Figure S7A). This is consistent with the presence of fewer ideal MAPK (Gonzalez et al., 1991) and GSK3 (Cohen and Frame, 2001) consensus sequences in the Smad2/3 linker (Figure S7B), and suggests that Acsl4a only affects the Bmp/Gdf, but not the Nodal/Activin/TGFβ subgroup of the TGFβ growth factor superfamily.

Another obvious question raised by our study is how Acsl4a activity ultimately works to suppress p38 MAPK and to activate Akt. While ACSL4 orthologs activate LC-PUFAs (the eicosanoid precursors), it is unclear whether loss of Acsl4a produces changes in eicosanoid signaling. Consistent with Acsl4a inhibiting MAPKs, LC-PUFAs and eicosanoid metabolites have been shown to regulate MAPK activity (Alexander et al., 2001; Denys et al., 2002; Garcia et al., 2009; Holzer et al., 2011; Rao et al., 2007; Schley et al., 2007; Xue

et al., 2006; Zeyda et al., 2003); however the mechanism(s) of MAPK regulation remains unclear. Holzer *et al* (2011) recently reported that membrane FA saturation levels impact JNK activity through c-Src activation. Saturated FAs activated JNK, while EPA inhibited JNK activity. Thus, Acsl4a activity could potentially influence levels of membrane phospholipids containing LC-PUFAs, which in turn alter membrane fluidity. Similarly, there is ample evidence for LC-PUFA and eicosanoid regulation of PI3K and Akt activity (Couplan et al., 2009; Covey et al., 2007; Hii et al., 2001). We have embarked on an extensive study to characterize zebrafish lipids during development with the eventual goal of exploring how specific lipid classes may change after Acsl4a genetic manipulation. These ongoing efforts will hopefully point to specific LC-PUFAs or their metabolites that regulate p38 and Akt activity, and thus, Bmp signaling. Future studies are needed to address whether p38 and Akt are required for dorsoventral patterning of the zebrafish embryo. Initial studies knocking down one of the six p38 orthologs (Hsu et al., 2011) and two of the five Akt orthologs (Cheng et al., 2013) (Jensen et al., 2010) report no dorsoventral patterning defects.

Our study reveals a mechanism by which an LC-PUFA activating enzyme modulates the Bmp signaling pathway. It is unlikely that the effect of Acsl4a on Bmp R-Smad activity is restricted to early dorsoventral patterning. Future studies will have to demonstrate whether similar mechanisms are at play during the other various roles of Bmp signaling during development and disease (Bandyopadhyay et al., 2013).

Experimental Procedures

Fish husbandry

Wild-type embryos were obtained from TL/EK, AB or FWT intercrosses. The FWT strain was generated from the AB strain outcrossed once to a wild-type strain from a commercial supplier (to reintroduce hybrid vigor) and inbred several generations. Embryos were collected from natural spawning and raised and staged as described (Kimmel et al., 1995). Embryos older than 15 hpf were anaesthetized with 0.2% Tricaine before use. Zebrafish care and experimental procedures were carried out in accordance with the Animal Care and Use Committees of both the Carnegie Institution and University of Cologne.

Whole-mount *in situ* hybridization

In situ hybridization was performed essentially as described (Hammerschmidt et al., 1996a; Thisse et al., 1993).

See Supplemental Methods for probe information.

Morpholinos and mRNA synthesis

MOs were purchased from Gene Tools, LLC. Unless otherwise stated, *acsl4a* MO1 was used in experiments. 5′ capped, 3′ polyadenylated mRNAs were synthesized using the mMESSAGE mMACHINE® kit (Ambion®).

For additional details see Supplemental Methods.

Phenotypic Analysis

Embryos were assigned a phenotypic class (Dorsalized: C5 most severe to C1 least severe; Ventralized: V4 most severe to V1 least severe; Wildtype: N) as previously described (Kishimoto et al., 1997).

Whole-mount immunohistochemistry

Whole-mount immunohistochemistry was performed essentially as described (Hammerschmidt et al., 1996b).

For additional details see Supplemental Methods.

Transplantation Studies

Donor embryos were injected at the 1–4 cell stage with fluorescent lineage tracer fluorescein dextran (1 mg/ml). Donor cells were transplanted into recipient embryos until high stage (3.5hpf). Embryos were fixed at 80% epiboly and immunofluorescence analyses were performed. Host embryos with one or, at maximum, two adjacent GFP positive cells at the ventral equatorial region were scored for nuclear pSmad$^{C\text{-}Term}$.

For pSmad$^{C\text{-}Term}$ quantification see Supplemental Methods.

Western Blots

Western blots and their subsequent quantification were performed by standard procedures (see Supplementary Methods).

Statistics

Bartlett's test was performed on all data to examine scedasticity prior to further statistical analysis. Unpaired student T-test was performed to compare normalized pSmad$^{C\text{-}Term}$ signal intensities of transplant data. ANOVA followed by the Dunnett post-hoc test was performed on the Bmp signaling pathway epistasis data (Figures 2,4, S5) and constitutively active AKT rescue data (Figure 6H). ANOVA with the REGWQ post-hoc test was carried out to evaluate the *acsl4a* mRNA rescue of *acsl4a* MO (Figure S2F). For Western blot analysis, one sample t-tests were performed on data normalized to control lysates (and for experiments with multiple comparisons, a Bonferroni correction factor was applied).

Supplementary Material

Refer to Web version on PubMed Central for supplementary material.

Acknowledgments

The authors are grateful to Marnie Halpern for editorial assistance and Amy Kowalski, Blake Caldwell and Evelin Fahle for technical assistance. We especially want to thank Michael Pickart and the scientists of the Zebrafish Functional Genomics Consortium, the NIH grant that instigated and helped fund this project, R01GM63904 (S.A.F. and M.H., PI Stephen Ekker). This work was also funded by a grant from NIH F31DK079421 (R.L.M.). The Carnegie Institution for Science endowment and the G. Harold and Leila Y. Mathers Charitable Foundation supported the laboratory of S.A.F. The German Research Foundation (DFG; SFB 572) and the European Union (7th Framework Program, Integrated Project ZF-HEALTH; HEALTH-F4-2010-242048) supported the laboratory of M.H.

References

Alexander LD, Cui XL, Falck JR, Douglas JG. Arachidonic acid directly activates members of the mitogen-activated protein kinase superfamily in rabbit proximal tubule cells. Kidney Int. 2001; 59:2039–2053. [PubMed: 11380805]

Bandyopadhyay A, Yadav PS, Prashar P. BMP signaling in development and diseases: a pharmacological perspective. Biochem Pharmacol. 2013; 85:857–864. [PubMed: 23333766]

Bauer H, Lele Z, Rauch GJ, Geisler R, Hammerschmidt M. The type I serine/threonine kinase receptor Alk8/Lost-a-fin is required for Bmp2b/7 signal transduction during dorsoventral patterning of the zebrafish embryo. Development. 2001; 128:849–858. [PubMed: 11222140]

Bazan NG. Cell survival matters: docosahexaenoic acid signaling, neuroprotection and photoreceptors. Trends Neurosci. 2006; 29:263–271. [PubMed: 16580739]

Bradham CA, McClay DR. p38 MAPK is essential for secondary axis specification and patterning in sea urchin embryos. Development. 2006; 133:21–32. [PubMed: 16319119]

Cao Y, Traer E, Zimmerman GA, McIntyre TM, Prescott SM. Cloning, expression, and chromosomal localization of human long-chain fatty acid-CoA ligase 4 (FACL4). Genomics. 1998; 49:327–330. [PubMed: 9598324]

Carvalho L, Heisenberg C-P. The yolk syncytial layer in early zebrafish development. Trends Cell Biol. 2010:586–592. [PubMed: 20674361]

Cheng YC, Hsieh FY, Chiang MC, Scotting PJ, Shih HY, Lin SJ, Wu HL, Lee HT. Akt1 mediates neuronal differentiation in zebrafish via a reciprocal interaction with notch signaling. PLoS ONE. 2013; 8:e54262. [PubMed: 23342113]

Cho Y. Abnormal Uterus with Polycysts, Accumulation of Uterine Prostaglandins, and Reduced Fertility in Mice Heterozygous for Acyl-CoA Synthetase 4 Deficiency. Biochem Biophys Res Commun. 2001; 284:993–997. [PubMed: 11409893]

Cohen P, Frame S. The renaissance of GSK3. Nat Rev Mol Cell Biol. 2001; 2:769–776. [PubMed: 11584304]

Coleman RA, Lewin TM, Muoio DM. Physiological and nutritional regulation of enzymes of triacylglycerol synthesis. Annu Rev Nutr. 2000; 20:77–103. [PubMed: 10940327]

Couplan E, Le Cann M, Le Foll C, Corporeau C, Blondel M, Delarue J. Polyunsaturated fatty acids inhibit PI3K activity in a yeast-based model system. Biotechnol J. 2009; 4:1190–1197. [PubMed: 19557793]

Covey TM, Edes K, Fitzpatrick FA. Akt activation by arachidonic acid metabolism occurs via oxidation and inactivation of PTEN tumor suppressor. Oncogene. 2007; 26:5784–5792. [PubMed: 17369849]

Cross DA, Alessi DR, Cohen P, Andjelkovich M, Hemmings BA. Inhibition of glycogen synthase kinase-3 by insulin mediated by protein kinase B. Nature. 1995; 378:785–789. [PubMed: 8524413]

De Robertis EM, Kuroda H. Dorsal-ventral patterning and neural induction in Xenopus embryos. Annu Rev Cell Dev Biol. 2004; 20:285–308. [PubMed: 15473842]

Denys A, Hichami A, Khan NA. Eicosapentaenoic acid and docosahexaenoic acid modulate MAP kinase enzyme activity in human T-cells. Mol Cell Biochem. 2002; 232:143–148. [PubMed: 12030372]

Eivers E, Fuentealba LC, De Robertis EM. Integrating positional information at the level of Smad1/5/8. Curr Opin Genet Dev. 2008; 18:304–310. [PubMed: 18590818]

Eivers E, Fuentealba LC, Sander V, Clemens JC, Hartnett L, De Robertis EM. Mad Is Required for Wingless Signaling in Wing Development and Segment Patterning in Drosophila. PLoS ONE. 2009; 4:e6543. [PubMed: 19657393]

Feldman B, Gates MA, Egan ES, Dougan ST, Rennebeck G, Sirotkin HI, Schier AF, Talbot WS. Zebrafish organizer development and germ-layer formation require nodal-related signals. Nature. 1998; 395:181–185. [PubMed: 9744277]

Fisher S, Amacher SL, Halpern ME. Loss of cerebum function ventralizes the zebrafish embryo. Development. 1997; 124:1301–1311. [PubMed: 9118801]

Fuentealba L, Eivers E, Ikeda A, Hurtado C, Kuroda H, Pera EM, De Robertis EM. Integrating patterning signals: Wnt/GSK3 regulates the duration of the BMP/Smad1 signal. Cell. 2007; 131:980–993. [PubMed: 18045539]

Funaba M, Zimmerman CM, Mathews LS. Modulation of Smad2-mediated signaling by extracellular signal-regulated kinase. The Journal of biological chemistry. 2002; 277:41361–41368. [PubMed: 12193595]

Fürthauer M, Van Celst J, Thisse C, Thisse B. Fgf signalling controls the dorsoventral patterning of the zebrafish embryo. Development. 2004; 131:2853–2864. [PubMed: 15151985]

Garcia MC, Ray DM, Lackford B, Rubino M, Olden K, Roberts JD. Arachidonic acid stimulates cell adhesion through a novel p38 MAPK-RhoA signaling pathway that involves heat shock protein 27. J Biol Chem. 2009; 284:20936–20945. [PubMed: 19506078]

Gazou A, Riess A, Grasshoff U, Schaferhoff K, Bonin M, Jauch A, Riess O, Tzschach A. Xq22.3-q23 deletion including ACSL4 in a patient with intellectual disability. Am J Med Genet A. 2013; 161:860–864. [PubMed: 23520119]

Gonzalez FA, Raden DL, Davis RJ. Identification of substrate recognition determinants for human ERK1 and ERK2 protein kinases. The Journal of biological chemistry. 1991; 266:22159–22163. [PubMed: 1939237]

Gritsman K, Zhang J, Cheng S, Heckscher E, Talbot WS, Schier AF. The EGF-CFC protein one-eyed pinhead is essential for nodal signaling. Cell. 1999; 97:121–132. [PubMed: 10199408]

Grossfield A, Feller SE, Pitman MC. A role for direct interactions in the modulation of rhodopsin by omega-3 polyunsaturated lipids. Proc Natl Acad Sci U S A. 2006; 103:4888–4893. [PubMed: 16547139]

Hammerschmidt M, Mullins MC. Dorsoventral patterning in the zebrafish: bone morphogenetic proteins and beyond. Results Probl Cell Differ. 2002; 40:72–95. [PubMed: 12353487]

Hammerschmidt M, Pelegri F, Mullins MC, Kane DA, van Eeden FJ, Granato M, Brand M, Furutani-Seiki M, Haffter P, Heisenberg CP, et al. dino and mercedes, two genes regulating dorsal development in the zebrafish embryo. Development. 1996a; 123:95–102. [PubMed: 9007232]

Hammerschmidt M, Serbedzija GN, McMahon AP. Genetic analysis of dorsoventral pattern formation in the zebrafish: requirement of a BMP-like ventralizing activity and its dorsal repressor. Genes Dev. 1996b; 10:2452–2461. [PubMed: 8843197]

Hashiguchi M, Mullins MC. Anteroposterior and dorsoventral patterning are coordinated by an identical patterning clock. Development. 2013; 140:1970–1980. [PubMed: 23536566]

He X, Saint-Jeannet JP, Woodgett JR, Varmus HE, Dawid IB. Glycogen synthase kinase-3 and dorsoventral patterning in Xenopus embryos. Nature. 1995; 374:617–622. [PubMed: 7715701]

Heasman J, Kofron M, Wylie C. Beta-catenin signaling activity dissected in the early Xenopus embryo: a novel antisense approach. Developmental Biology. 2000; 222:124–134. [PubMed: 10885751]

Hii CS, Moghadammi N, Dunbar A, Ferrante A. Activation of the phosphatidylinositol 3-kinase-Akt/protein kinase B signaling pathway in arachidonic acid-stimulated human myeloid and endothelial cells: involvement of the ErbB receptor family. The Journal of biological chemistry. 2001; 276:27246–27255. [PubMed: 11359783]

Hild M, Dick A, Rauch GJ, Meier A, Bouwmeester T, Haffter P, Hammerschmidt M. The smad5 mutation somitabun blocks Bmp2b signaling during early dorsoventral patterning of the zebrafish embryo. Development. 1999; 126:2149–2159. [PubMed: 10207140]

Holzer, Ryan G.; Park, EJ.; Li, N.; Tran, H.; Chen, M.; Choi, C.; Solinas, G.; Karin, M. Saturated Fatty Acids Induce c-Src Clustering within Membrane Subdomains, Leading to JNK Activation. Cell. 2011; 147:173–184. [PubMed: 21962514]

Hsu RJ, Lin CC, Su YF, Tsai HJ. dickkopf-3-related gene regulates the expression of zebrafish myf5 gene through phosphorylated p38a-dependent Smad4 activity. The Journal of biological chemistry. 2011; 286:6855–6864. [PubMed: 21159776]

Jensen PJ, Gunter LB, Carayannopoulos MO. Akt2 modulates glucose availability and downstream apoptotic pathways during development. The Journal of biological chemistry. 2010; 285:17673–17680. [PubMed: 20356836]

Jia S, Ren Z, Li X, Zheng Y, Meng A. smad2 and smad3 are required for mesendoderm induction by transforming growth factor-beta/nodal signals in zebrafish. The Journal of biological chemistry. 2008; 283:2418–2426. [PubMed: 18025082]

Kamaraju AK, Roberts AB. Role of Rho/ROCK and p38 MAP kinase pathways in transforming growth factor-beta-mediated Smad-dependent growth inhibition of human breast carcinoma cells in vivo. J Biol Chem. 2005; 280:1024–1036. [PubMed: 15520018]

Kamato D, Burch ML, Piva TJ, Rezaei HB, Rostam MA, Xu S, Zheng W, Little PJ, Osman N. Transforming growth factor-beta signalling: Role and consequences of Smad linker region phosphorylation. Cell Signal. 2013; 25:2017–2024. [PubMed: 23770288]

Kang MJ, Fujino T, Sasano H, Minekura H, Yabuki N, Nagura H, Iijima H, Yamamoto TT. A novel arachidonate-preferring acyl-CoA synthetase is present in steroidogenic cells of the rat adrenal, ovary, and testis. Proc Natl Acad Sci USA. 1997; 94:2880–2884. [PubMed: 9096315]

Keren A, Keren-Politansky A, Bengal E. A p38 MAPK-CREB pathway functions to pattern mesoderm in Xenopus. Developmental Biology. 2008; 322:86–94. [PubMed: 18675264]

Kimmel C, Ballard W, Kimmel S, Ullmann B, Schilling T. Stages of embryonic development of the zebrafish. Dev Dyn. 1995; 203:253–310. [PubMed: 8589427]

Kimmel CB, Warga RM, Schilling TF. Origin and organization of the zebrafish fate map. Development. 1990; 108:581–594. [PubMed: 2387237]

Kishimoto Y, Lee KH, Zon L, Hammerschmidt M, Schulte-Merker S. The molecular nature of zebrafish swirl: BMP2 function is essential during early dorsoventral patterning. Development. 1997; 124:4457–4466. [PubMed: 9409664]

Kitajka K, Puskas LG, Zvara A, Hackler L Jr, Barcelo-Coblijn G, Yeo YK, Farkas T. The role of n-3 polyunsaturated fatty acids in brain: modulation of rat brain gene expression by dietary n-3 fatty acids. Proc Natl Acad Sci U S A. 2002; 99:2619–2624. [PubMed: 11880617]

Kohn AD, Summers SA, Birnbaum MJ, Roth RA. Expression of a constitutively active Akt Ser/Thr kinase in 3T3-L1 adipocytes stimulates glucose uptake and glucose transporter 4 translocation. The Journal of biological chemistry. 1996; 271:31372–31378. [PubMed: 8940145]

Kramer C, Mayr T, Nowak M, Schumacher J, Runke G, Bauer H, Wagner D, Schmid B, Imai Y, Talbot W. Maternally Supplied Smad5 Is Required for Ventral Specification in Zebrafish Embryos Prior to Zygotic Bmp Signaling. Developmental Biology. 2002; 250:263–279. [PubMed: 12376102]

Kretzschmar M, Doody J, Massagué J. Opposing BMP and EGF signalling pathways converge on the TGF-beta family mediator Smad1. Nature. 1997; 389:618–622. [PubMed: 9335504]

Kretzschmar M, Doody J, Timokhina I, Massague J. A mechanism of repression of TGFbeta/Smad signaling by oncogenic Ras. Genes & Development. 1999; 13:804–816. [PubMed: 10197981]

Lekven AC, Thorpe CJ, Waxman JS, Moon RT. Zebrafish wnt8 encodes two wnt8 proteins on a bicistronic transcript and is required for mesoderm and neurectoderm patterning. Dev Cell. 2001; 1:103–114. [PubMed: 11703928]

Little SC, Mullins MC. Extracellular modulation of BMP activity in patterning the dorsoventral axis. Birth Defects Res C Embryo Today. 2006; 78:224–242. [PubMed: 17061292]

Liu Z, Huang Y, Zhang Y, Chen D, Zhang YQ. Drosophila Acyl-CoA synthetase long-chain family member 4 regulates axonal transport of synaptic vesicles and is required for synaptic development and transmission. Journal of Neuroscience. 2011; 31:2052–2063. [PubMed: 21307243]

Longo I, Frints SGM, Fryns JP, Meloni I, Pescucci C, Ariani F, Borghgraef M, Raynaud M, Marynen P, Schwartz C, et al. A third MRX family (MRX68) is the result of mutation in the long chain fatty acid-CoA ligase 4 (FACL4) gene: proposal of a rapid enzymatic assay for screening mentally retarded patients. J Med Genet. 2003; 40:11–17. [PubMed: 12525535]

Macias-Silva M, Abdollah S, Hoodless PA, Pirone R, Attisano L, Wrana JL. MADR2 is a substrate of the TGFbeta receptor and its phosphorylation is required for nuclear accumulation and signaling. Cell. 1996; 87:1215–1224. [PubMed: 8980228]

McQuilton P, St Pierre SE, Thurmond J. Consortium tF. FlyBase 101 - the basics of navigating FlyBase. Nucleic Acids Res. 2012; 40:D706–D714. [PubMed: 22127867]

Medina M, Wandosell F. Deconstructing GSK-3: The Fine Regulation of Its Activity. Int J Alzheimers Dis. 2011; 2011:479249. [PubMed: 21629747]

Meloni I, Muscettola M, Raynaud M, Longo I, Bruttini M, Moizard MP, Gomot M, Chelly J, des Portes V, Fryns JP, et al. FACL4, encoding fatty acid-CoA ligase 4, is mutated in nonspecific X-linked mental retardation. Nat Genet. 2002a; 30:436–440. [PubMed: 11889465]

Meloni I, Parri V, De Filippis R, Ariani F, Artuso R, Bruttini M, Katzaki E, Longo I, Mari F, Bellan C, et al. The XLMR gene ACSL4 plays a role in dendritic spine architecture. NSC. 2009; 159:657–669.

Meloni I, Vitelli F, Pucci L, Lowry RB, Tonlorenzi R, Rossi E, Ventura M, Rizzoni G, Kashtan CE, Pober B, et al. Alport syndrome and mental retardation: clinical and genetic dissection of the contiguous gene deletion syndrome in Xq22.3 (ATS-MR). J Med Genet. 2002b; 39:359–365. [PubMed: 12011158]

Mintzer KA, Lee MA, Runke G, Trout J, Whitman M, Mullins MC. Lost-a-fin encodes a type I BMP receptor, Alk8, acting maternally and zygotically in dorsoventral pattern formation. Development. 2001; 128:859–869. [PubMed: 11222141]

Mori S, Matsuzaki K, Yoshida K, Furukawa F, Tahashi Y, Yamagata H, Sekimoto G, Seki T, Matsui H, Nishizawa M, et al. TGF-beta and HGF transmit the signals through JNK-dependent Smad2/3 phosphorylation at the linker regions. Oncogene. 2004; 23:7416–7429. [PubMed: 15326485]

Mullins MC, Hammerschmidt M, Kane DA, Odenthal J, Brand M, van Eeden FJ, Furutani-Seiki M, Granato M, Haffter P, Heisenberg CP, et al. Genes establishing dorsoventral pattern formation in the zebrafish embryo: the ventral specifying genes. Development. 1996; 123:81–93. [PubMed: 9007231]

Nasevicius A, Ekker SC. Effective targeted gene 'knockdown' in zebrafish. Nat Genet. 2000; 26:216–220. [PubMed: 11017081]

Nguyen VH, Schmid B, Trout J, Connors SA, Ekker M, Mullins MC. Ventral and lateral regions of the zebrafish gastrula, including the neural crest progenitors, are established by a bmp2b/swirl pathway of genes. Developmental Biology. 1998; 199:93–110. [PubMed: 9676195]

Nikaido M, Tada M, Takeda H, Kuroiwa A, Ueno N. In vivo analysis of variants of zebrafish BMPR-IA: range of action and involvement of BMP in ectoderm patterning. Development. 1999; 126:181–190. [PubMed: 9834197]

Pera EM. Integration of IGF, FGF, and anti-BMP signals via Smad1 phosphorylation in neural induction. Genes & Development. 2003; 17:3023–3028. [PubMed: 14701872]

Perdiguero E, Sousa-Victor P, Ruiz-Bonilla V, Jardi M, Caelles C, Serrano AL, Munoz-Canoves P. p38/MKP-1-regulated AKT coordinates macrophage transitions and resolution of inflammation during tissue repair. J Cell Biol. 2011; 195:307–322. [PubMed: 21987635]

Piccini M, Vitelli F, Bruttini M, Pober BR, Jonsson JJ, Villanova M, Zollo M, Borsani G, Ballabio A, Renieri A. FACL4, a new gene encoding long-chain acyl-CoA synthetase 4, is deleted in a family with Alport syndrome, elliptocytosis, and mental retardation. Genomics. 1998; 47:350–358. [PubMed: 9480748]

Rao JS, Ertley RN, Lee HJ, Demar JC, Arnold JT, Rapoport SI, Bazinet RP. n-3 Polyunsaturated fatty acid deprivation in rats decreases frontal cortex BDNF via a p38 MAPK-dependent mechanism. Mol Psychiatry. 2007; 12:36–46. [PubMed: 16983391]

Raynaud M, Moizard MP, Dessay B, Briault S, Toutain A, Gendrot C, Ronce N, Moraine C. Systematic analysis of X-inactivation in 19XLMR families: extremely skewed profiles in carriers in three families. Eur J Hum Genet. 2000; 8:253–258. [PubMed: 10854107]

Rui Y, Xu Z, Xiong B, Cao Y, Lin S, Zhang M, Chan SC, Luo W, Han Y, Lu Z, et al. A beta-catenin-independent dorsalization pathway activated by Axin/JNK signaling and antagonized by aida. Dev Cell. 2007; 13:268–282. [PubMed: 17681137]

Sapkota G, Alarcón C, Spagnoli FM, Brivanlou AH, Massagué J. Balancing BMP signaling through integrated inputs into the Smad1 linker. Mol Cell. 2007; 25:441–454. [PubMed: 17289590]

Schier AF, Talbot WS. Molecular genetics of axis formation in zebrafish. Annu Rev Genet. 2005; 39:561–613. [PubMed: 16285872]

Schley PD, Brindley DN, Field CJ. (n-3) PUFA alter raft lipid composition and decrease epidermal growth factor receptor levels in lipid rafts of human breast cancer cells. J Nutr. 2007; 137:548–553. [PubMed: 17311938]

Sidi S, Goutel C, Peyriéras N, Rosa FM. Maternal induction of ventral fate by zebrafish radar. Proc Natl Acad Sci USA. 2003; 100:3315–3320. [PubMed: 12601179]

Stillwell W, Shaikh SR, Zerouga M, Siddiqui R, Wassall SR. Docosahexaenoic acid affects cell signaling by altering lipid rafts. Reprod Nutr Dev. 2005; 45:559–579. [PubMed: 16188208]

Stinnett L, Lewin TM, Coleman RA. Mutagenesis of rat acyl-CoA synthetase 4 indicates amino acids that contribute to fatty acid binding. Biochim Biophys Acta. 2007; 1771:119–125. [PubMed: 17110164]

Tanimoto H, Itoh S, ten Dijke P, Tabata T. Hedgehog creates a gradient of DPP activity in Drosophila wing imaginal discs. Mol Cell. 2000; 5:59–71. [PubMed: 10678169]

Thisse C, Thisse B, Schilling T, Postlethwait J. Structure of the zebrafish snail1 gene and its expression in wild-type, spadetail and no tail mutant embryos. Development. 1993; 119:1203–1215. [PubMed: 8306883]

Thornton TM, Pedraza-Alva G, Deng B, Wood CD, Aronshtam A, Clements JL, Sabio G, Davis RJ, Matthews DE, Doble B, et al. Phosphorylation by p38 MAPK as an alternative pathway for GSK3beta inactivation. Science. 2008; 320:667–670. [PubMed: 18451303]

Wieser R, Wrana JL, Massague J. GS domain mutations that constitutively activate T beta R-I, the downstream signaling component in the TGF-beta receptor complex. The EMBO journal. 1995; 14:2199–2208. [PubMed: 7774578]

Wilm TP, Solnica-Krezel L. Radar breaks the fog: insights into dorsoventral patterning in zebrafish. Proc Natl Acad Sci U S A. 2003; 100:4363–4365. [PubMed: 12682283]

Xue H, Wan M, Song D, Li Y, Li J. Eicosapentaenoic acid and docosahexaenoic acid modulate mitogen-activated protein kinase activity in endothelium. Vascul Pharmacol. 2006; 44:434–439. [PubMed: 16616699]

Yonath H, Marek-Yagel D, Resnik-Wolf H, Abu-Horvitz A, Baris HN, Shohat M, Frydman M, Pras E. X inactivation testing for identifying a non-syndromic X-linked mental retardation gene. J Appl Genet. 2011; 52:437–441. [PubMed: 21584729]

Zeyda M, Szekeres AB, Säemann MD, Geyeregger R, Stockinger H, Zlabinger GJ, Waldhäusl W, Stulnig TM. Suppression of T cell signaling by polyunsaturated fatty acids: selectivity in inhibition of mitogen-activated protein kinase and nuclear factor activation. J Immunol. 2003; 170:6033–6039. [PubMed: 12794131]

Zhang Y, Chen D, Wang Z. Analyses of mental dysfunction-related ACSl4 in Drosophila reveal its requirement for Dpp/BMP production and visual wiring in the brain. Human Molecular Genetics. 2009; 18:3894–3905. [PubMed: 19617635]

Zhang Y, Gao Y, Zhao X, Wang Z. Drosophila long-chain acyl-CoA synthetase acts like a gap gene in embryonic segmentation. Developmental Biology. 2011; 353:259–265. [PubMed: 21385576]

Zhang YE. Non-Smad pathways in TGF-beta signaling. Cell Res. 2009; 19:128–139. [PubMed: 19114990]

Zhu H, Kavsak P, Abdollah S, Wrana JL, Thomsen GH. A SMAD ubiquitin ligase targets the BMP pathway and affects embryonic pattern formation. Nature. 1999; 400:687–693. [PubMed: 10458166]

Highlights

- PUFA-modifying enzyme, Acsl4a, is essential for zebrafish dorsoventral patterning
- Acsl4a enhances Bmp signaling via stabilization of Bmp-Smad transcription factors
- Acsl4a loss activates p38 and GSK3, resulting in Smad phosphorylation and degradation
- Ascl4a inhibits GSK3 via activation of AKT

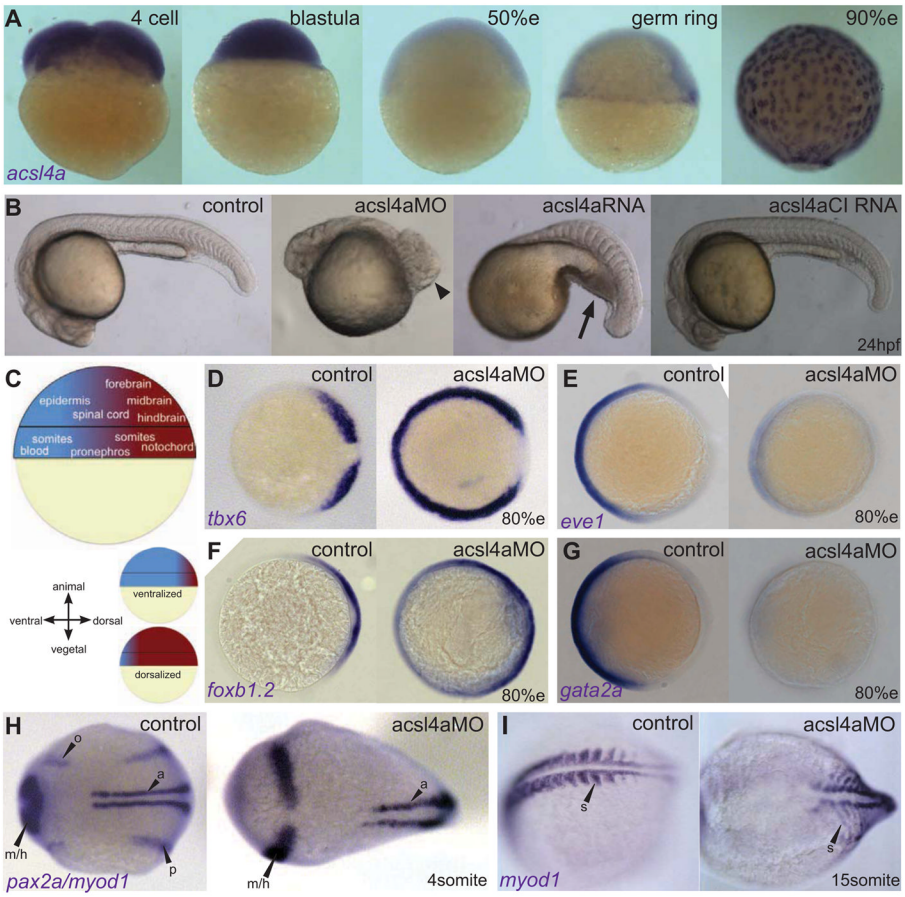

Figure 1. Acsl4a is necessary for proper dorsoventral patterning

(A) *acsl4a* expression throughout early embryonic development. Whole-mount mRNA *in situ* hybridizations. Expression pattern was consistent over multiple experiments (n=7) and between 2 separate riboprobes targeting *acsl4a*. Lateral views, animal pole to the top. e:epiboly.

(B) Morphological defects in dorsoventral patterning caused by perturbation of *acsl4a* expression. Representative bright-field images of wild-type embryos (24 hpf) that are dorsalized (class C4 phenotype shown) when injected with *acsl4a* MO and ventralized (class V3 phenotype shown) when injected with *acsl4a* mRNA. Embryos injected with a catalytically-inactive version of *acsl4a* (acsl4aCI) mRNA and control siblings develop normally. Arrowhead indicates wound-up trunk and arrow indicates expanded blood island. 500fmol *acsl4a* MO: n=8 experiments (406 embryos). Phenotypic classes were assigned as described by (Kishimoto et al., 1997) 79%C5, 8%C4, 11%C3, 1%C2, 1%C1. 1.2–1.5 ng *acsl4a* mRNA; n=3 (101 embryos); 6%V4, 23%V3, 25%V2, 45%V1, 2%N. 1.2–1.5 ng *acsl4aCI* mRNA; n=3 (123 embryos); 100% N.

(C) Fate map of the gastrula-stage zebrafish embryo (Kimmel et al., 1990; Schier and Talbot, 2005). Blue represents ventral fates and red represents dorsal fates.

(D–G) Whole mount mRNA *in situ* hybridization of markers of dorsal and ventral tissues in 80% epiboly stage embryos, either control or *acsl4a* MO-injected. Animal pole view, dorsal to the right.

(D) *tbx6*, a marker of dorsal presumptive paraxial mesoderm, is expanded ventrally in *acsl4a* MO-injected embryos. 95% of *acsl4a* MO-injected (750 fmol) embryos displayed expansion >180 degrees (n=8, 323 embryos).

(E) *eve1*, a marker of ventral mesoderm, is reduced in *acsl4a* MO-injected (500 fmol) embryos (97%; n=6, 272 embryos).
(F) *foxb1.2*, a marker of neural plate/dorsal ectoderm, is expanded ventrally in *acsl4a* MO-injected (500 fmol) embryos (93%; n=4, 135 embryos).
(G) *gata2a*, a marker for epidermis/ventral ectoderm, is reduced in *acsl4a* MO-injected (500 fmol) embryos (98%; n=4, 181 embryos).
(H) *pax2a* and *myod1* expression in 4-somite stage embryos. Dorsal view, anterior to the left. *pax2a* marks m/h: midbrain/hindbrain boundary, o: otic placode, p: pronephros. *myod1* marks a: adaxial cells. 98% of *acsl4a* MO-injected (500 fmol) embryos had expansion of *pax2a* marking m/h (n=7, 125 embryos). 75% of *acsl4a* MO-injected (500 fmol) embryos had loss and 25% had reduced expression of *pax2a* marking pronephros (n=5, 86 embryos).
(I) *myod1* expression in 15-somite stage embryos. Dorsal view, anterior to the left. s: somites. 96% of *acsl4a* MO-injected (500 fmol) embryos had expanded somites (n=10, 138 embryos).
See also Figures S1 and S2.

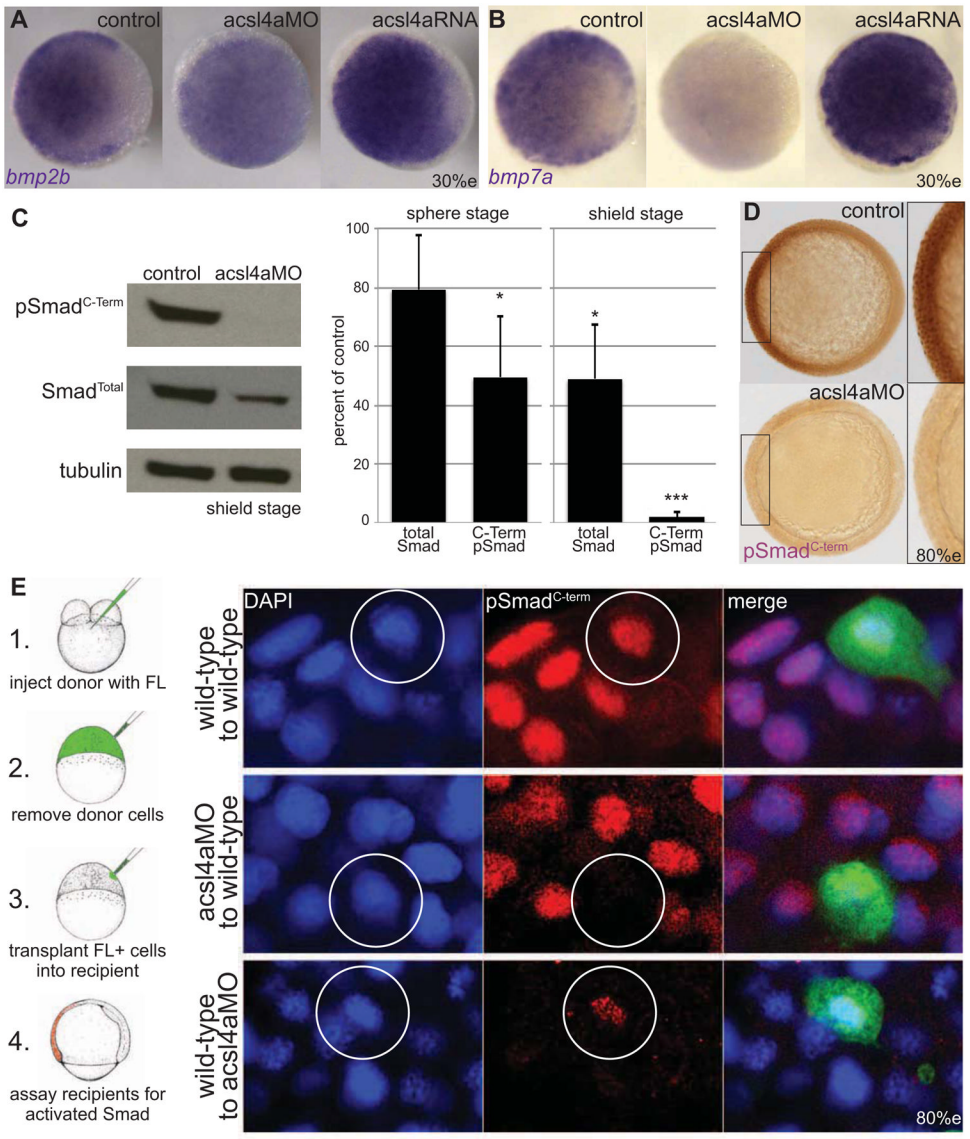

Figure 2. Bmp expression and signaling is dependent on Acsl4a

(A–B) Whole-mount mRNA *in situ* hybridization of *bmp* transcripts in control embryos and embryos injected with *acls4a* MO (500 fmol) or *acsl4a* mRNA (1.25 ng). In *acls4a* morphants, the ventral to dorsal gradient of (A) *bmp2b* and (B) *bmp7a* is attenuated (in 87% and 78%, respectively) *acls4a* while overexpression enhances *bmp* expression (in 77% and 75%, respectively). n=4, 88–119 embryos. Animal pole view, dorsal to the right (30% epiboly).

(C) (Left) Western blot of C-terminally phosphorylated Smad1/5/8 ($pSmad^{C\text{-}Term}$) and total Smad1/5/8 ($Smad^{Total}$) from shield-stage control embryos and embryos injected with 750 fmol *acsl4a* MO. (Right) Quantification of 3 (sphere) or 5 (shield) experiments. Data are represented as mean ± SE * $p<0.05$ *** $p<0.001$; one sample t-test with Bonferroni correction (sphere stage MO=500 fmol, shield stage MO=500–750 fmol).

(D) Whole-mount immunostain against $pSmad^{C\text{-}Term}$ at 80% epiboly. Staining is reduced in morphants (500 fmol) when compared to control siblings (98%; n=5, 155 embryos). Animal pole view, dorsal to the right (80% epiboly). Inset is a 2X magnification of the ventral-most region.

(E) Acsl4a is needed in the Bmp ligand-receiving cell for Smad activation. (Left) Schematic of transplantation experiment. (Right) pSmad$^{C\text{-}Term}$ immunofluorescence in transplanted cells in ventral equatorial regions of host embryos (80% epiboly). Top panel: wild-type cells transplanted into wild-type embryos have normal pSmad$^{C\text{-}Term}$ staining (26/26 embryos, three independent experiments). Middle panel: Morphant cells transplanted into wild-type embryos lack pSmad$^{C\text{-}Term}$ staining, whereas adjacent cells have normal pSmad$^{C\text{-}Term}$ staining (16/16 embryos, n=3). Bottom panel: Wild-type cells transplanted into morphants have pSmad$^{C\text{-}Term}$ staining, whereas adjacent morphant cells lack pSmad$^{C\text{-}Term}$ signals (17/17 embryos, n=3). Wild-type cells transplanted into morphants show reduced pSmad$^{C\text{-}Term}$ staining compared to wild-type cells transplanted into wild-type hosts (compare bottom and top panels). FL: Fluorescein dextran.
See also Figure S3.

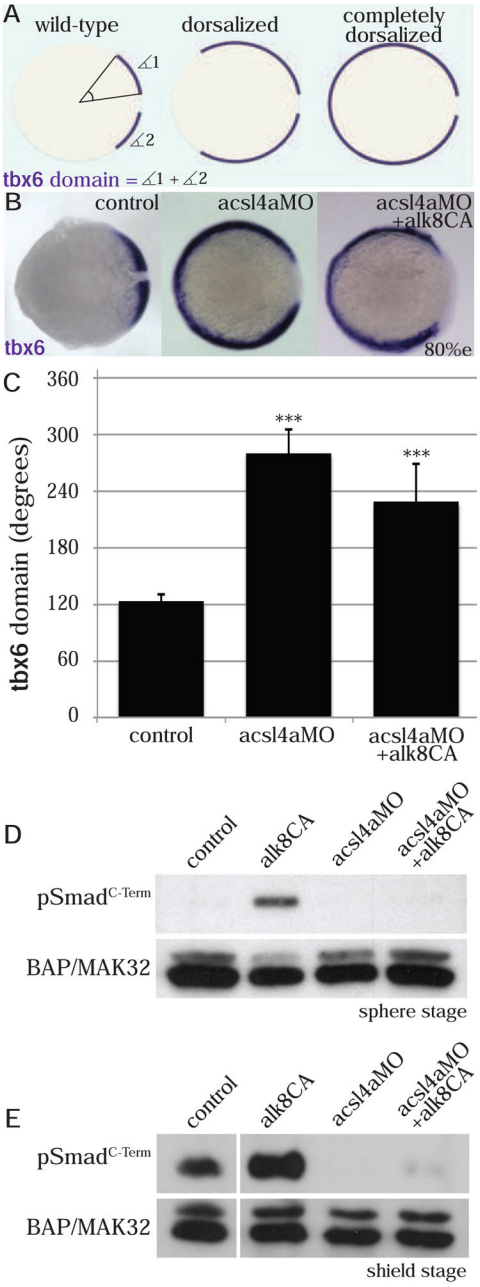

Figure 3. Acsl4a acts downstream of Bmp receptor activation

(A) The extent of dorsalization is measured by adding the angles of the arcs of dorsal marker *tbx6* expression on either side of the *tbx6* negative midline at 80% epiboly. Embryos are considered completely dorsalized if the arcs meet on the ventral side.

(B–C) Constitutively active Bmp receptor does not rescue the phenotype caused by *acsl4a* depletion.

(B) *tbx6* expression in a control embryo, embryo injected with *acsl4a* MO alone (750 fmol), or *acsl4a* MO combined with constitutively active *alk8* (alk8CA, 1.5 ng) mRNA. Vegetal pole view, dorsal to the right (80% epiboly).

(C) Quantification of *tbx6* expression domain. Data are represented as mean of experimental means ± pooled SE (n=3–8, 12–80 embryos/experiment). ANOVA with Dunnett post-hoc test; *** $p<0.0001$, compared to control.
(D–E) Western blots (n=3) of C-terminally phosphorylated Smad1/5/8 ($pSmad^{C\text{-}Term}$) from embryos injected with *alk8CA* mRNA (20–40 pg), *acsl4a* MO (500 fmol), or *acsl4a* MOand *alk8CA* mRNA combined. Anti-BAP/MAK32 is the loading control. (D) Lysates from sphere-stage embryos. (E) Lysates from shield-stage embryos. An extraneous lane between control and *alk8CA* is omitted.
See also Figure S4.

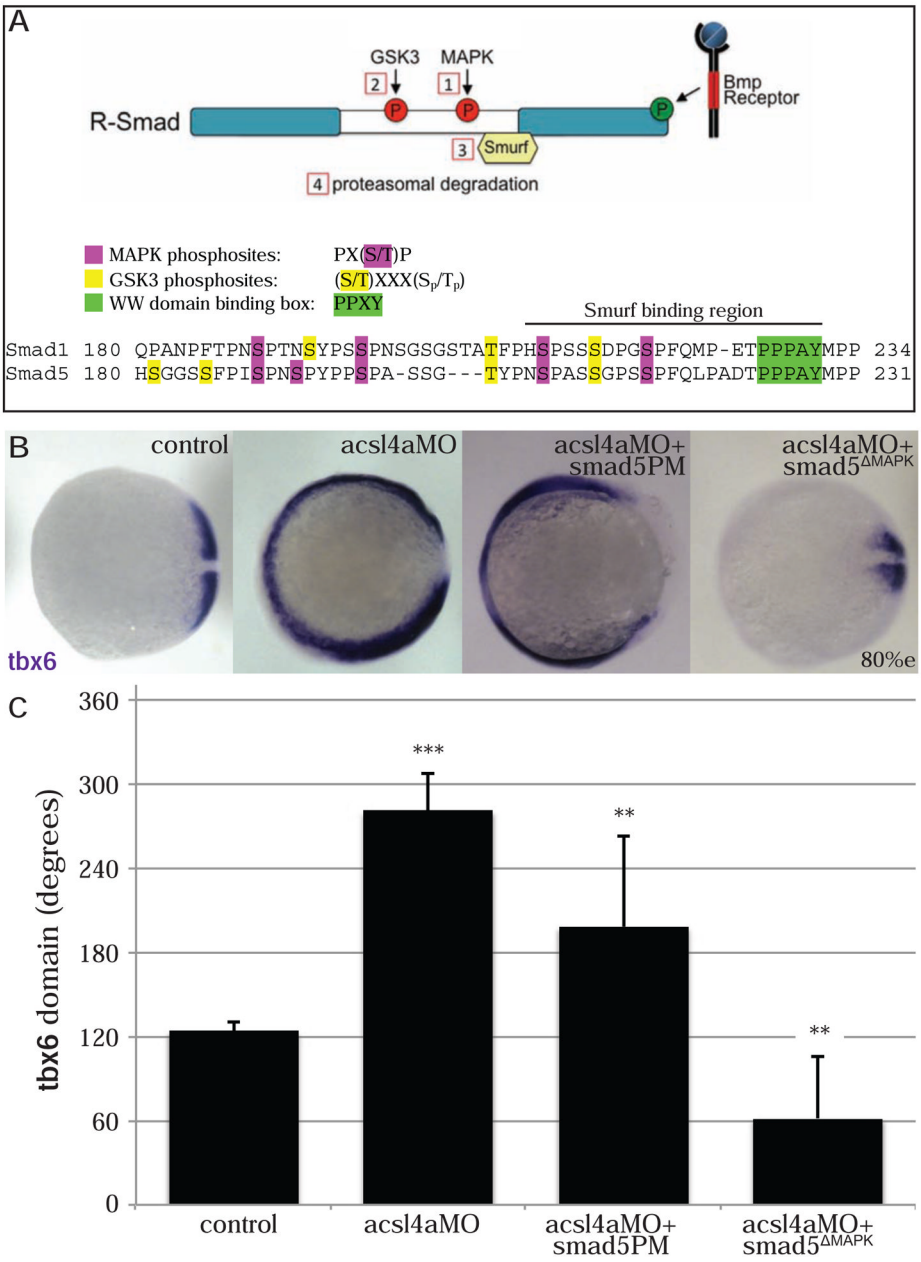

Figure 4. Acsl4a acts via R-Smad phosphorylation at MAPK consensus sites

(A) Model of R-Smad regulation by phosphorylation. (Top) The Bmp receptor positively regulates (green) R-Smad activity by phosphorylating the C-terminus. Negative regulation (red) of R-Smad occurs in sequential steps: 1) MAPK phosphorylates the R-Smad linker. 2) GSK3 phosphorylates the linker upstream of MAPK phosphoresidues. 3) Smurf1/2 E3 ubiquitin ligase recognizes R-Smad after phosphorylation by MAPK and/or GSK3. 4) Smurf1/2 polyubiquitinates R-Smad, leading to its proteasomal degradation. (Bottom) Sequence alignment of zebrafish Smad1 and Smad5 linker regions with important residues highlighted.

(B) *tbx6* expression in a control embryo, embryo injected with *acsl4a* MO alone (750 fmol), *acsl4a* MO combined with a C-terminal phosphomimic *smad5* mRNA (smad5PM; 1.5 ng),

and *acsl4a* MO combined with a MAPK-insensitive version of *smad5* mRNA (smad5$^{\Delta MAPK}$; 1.5 ng). Vegetal pole view, dorsal to the right (80% epiboly).
(C) Quantification of *tbx6* expression domain. Data are represented as mean of experimental means ± pooled SE (n=3–8, 12–80 embryos/experiment). ANOVA with Dunnett post-hoc test; * $p<0.01$, ** $p \leq 0.005$, *** $p<0.0001$; compared to control.
See also Figures S5.

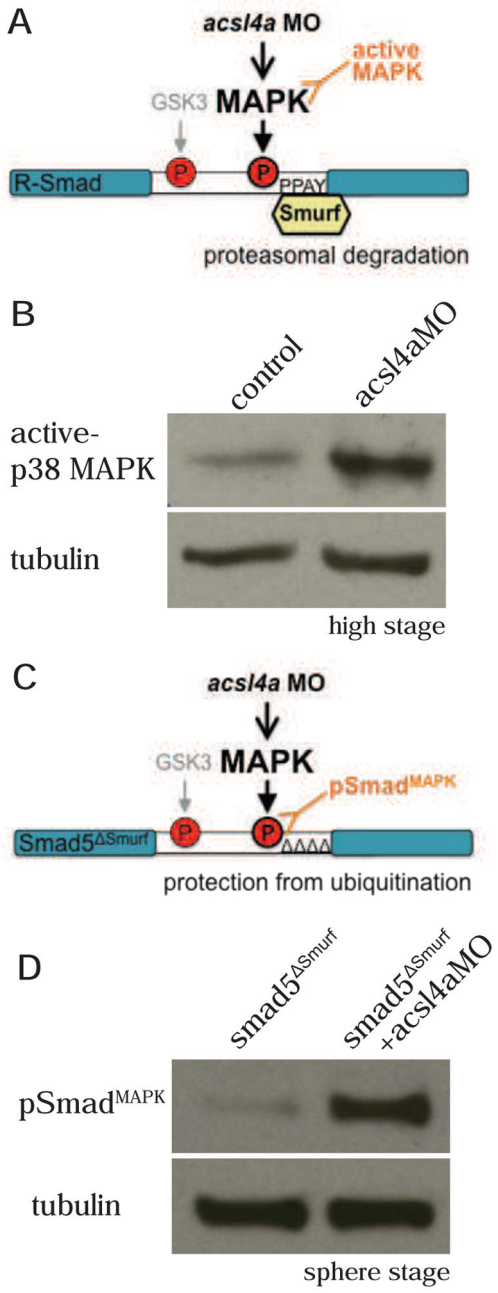

Figure 5. Acsl4a regulates p38 MAPK activity and R-Smad linker phosphorylation

(A) An *acsl4a* MO-dependent increase in MAPK activity would result in phosphorylation of R-Smad and recruitment of Smurf ubiquitin ligase. An increase in MAPK activity can be assayed by antibodies specific to activated MAPK.

(B) p38 MAPK activity is upregulated in *acsl4a* morphants (750 fmol) at high stage. Western blot for phosphorylated (Thr^{180}/Tyr^{182}) p38 MAPK (active-p38 MAPK; n=6).

(C) $Smad5^{\Delta Smurf}$ lacks the WW domain-binding box (PPPAY⇒ΔΔΔΔΔ) recognized by Smurf E3 ubiquitin ligase, thus it is prevented from linker-mediated degradation. An increase in MAPK phosphorylation of R-Smad can be assayed with a phospho-specific antibody, $pSmad^{MAPK}$.

(D) Smad5$^{\Delta Smurf}$ is phosphorylated at the MAPK consensus site (Ser^{215}) after *acsl4a* knock down. Western blot for MAPK phosphorylated Smad (pSmad^{MAPK}; gift of de Robertis) at sphere stage. *acsl4a* MO injection (750 fmol) results in increased pSmad^{MAPK} staining. Alpha tubulin is the loading control.
See also Figure S6.

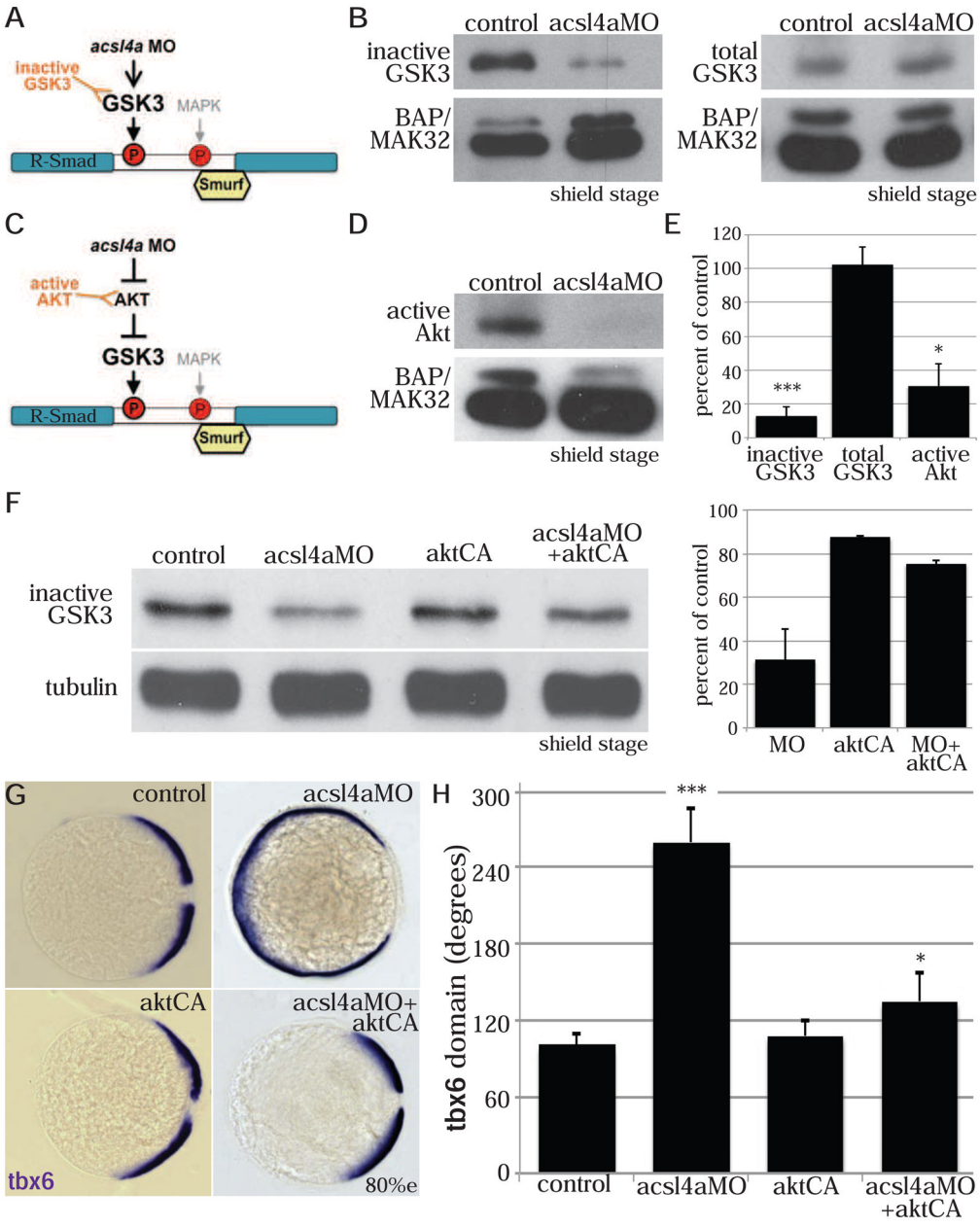

Figure 6. Acsl4a regulates GSK3 activity

(A) An *acsl4a* MO-dependent increase in GSK3 activity would result in phosphorylation of R-Smad and recruitment of Smurf ubiquitin ligase. There are inhibitory phosphorylation sites (GSK3α Ser^{21}/GSK3β Ser^{9}) that control GSK3 activity level, thus an antibody that recognizes the inhibitory phosphorylation (inactive GSK3) can assay GSK3 activity.

(B) GSK3 activity is increased in *acsl4a* morphants (500 fmol). (Left) Western blot for inhibitory phosphorylation (GSK3α Ser^{21}/GSK3β Ser^{9}) of GSK3 (inactive GSK3). (Right) Western blot for total GSK3β. BAP/MAK32 is the loading control.

(C) GSK3 is inhibited by Akt. An *acsl4a* MO-dependent decrease in Akt activity would result in decreased inhibition (thus activation) of GSK3. A decrease in Akt activity can be assayed by an antibody specific to active (phosphorylated on Ser^{473}) Akt.

(D) Akt activity is decreased in *acsl4a* morphants (500 fmol). Western blot for phosphorylated (Ser^{473}) Akt (active AKT). BAP/MAK32 is the loading control.
(E) Quantification of blots (B&D). Data is mean ± SE of 3–4 experiments and represented as percent of control (* $p<.05$ *** $p<0.001$; one sample t-test with Bonferroni correction).
(F–H) Constitutively active, myristoylated Akt rescues the *acsl4a* MO's dorsalized phenotype.
(F) Constitutively active Akt (50–100 pg) decreases GSK3 activity (increase in inactive GSK3) in acsl4a MO-injected (333 fmol) embryos. Data are represented as mean ± SD (n=2).
(G) Expression of *tbx6* in a control embryo, embryo injected with *acsl4a* MO alone (333 fmol), embryo injected with constitutively active akt (50–100 pg; aktCA), and *acsl4a* MO with aktCA. Vegetal pole view, dorsal to the right (80% epiboly).
(H) Quantification of *tbx6* expression domain. Data are represented as mean of experimental means ± pooled SE (n=3, 20–24 embryos/experiment). ANOVA with Dunnett; * $p<0.05$, *** $p<0.0001$.

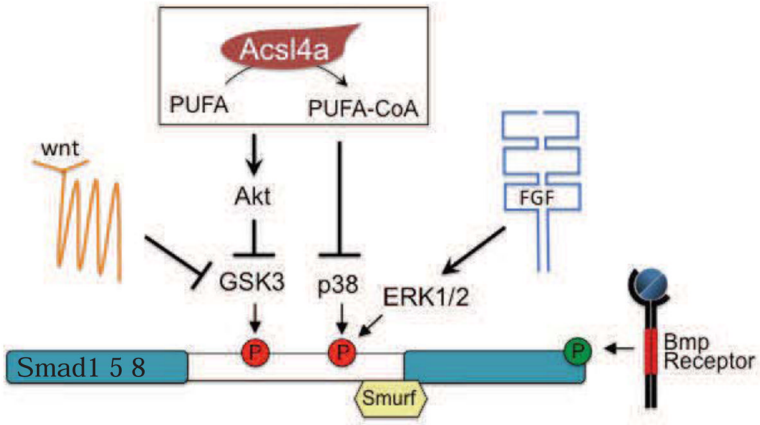

Figure 7. Acsl4a enzyme activity, Wnt signaling and FGF signaling regulate R-Smads via parallel pathways

See also Figure S7.